

Dendritic pathology, spine loss and synaptic reorganization in human cortex from epilepsy patients

Laura Rossini,¹ Dalia De Santis,¹ Roberta Rosa Mauceri,¹ Chiara Tesoriero,² Marina Bentivoglio,² Emanuela Maderna,³ Antonio Maiorana,⁴ Francesco Deleo,¹ Marco de Curtis,¹ Giovanni Tringali,⁵ Massimo Cossu,⁶ Gemma Tumminelli,⁶ Manuela Bramerio,⁷ Roberto Spreafico,¹ Laura Tassi⁶ and Rita Garbelli¹

Neuronal dendritic arborizations and dendritic spines are crucial for a normal synaptic transmission and may be critically involved in the pathophysiology of epilepsy. Alterations in dendritic morphology and spine loss mainly in hippocampal neurons have been reported both in epilepsy animal models and in human brain tissues from patients with epilepsy. However, it is still unclear whether these dendritic abnormalities relate to the cause of epilepsy or are generated by seizure recurrence. We investigated fine neuronal structures at the level of dendritic and spine organization using Golgi impregnation, and analysed synaptic networks with immunohistochemical markers of glutamatergic (vGLUT1) and GABAergic (vGAT) axon terminals in human cerebral cortices derived from epilepsy surgery. Specimens were obtained from 28 patients with different neuropathologically defined aetiologies: type Ia and type II focal cortical dysplasia, cryptogenic (no lesion) and temporal lobe epilepsy with hippocampal sclerosis. Autoptic tissues were used for comparison. Three-dimensional reconstructions of Golgi-impregnated neurons revealed severe dendritic reshaping and spine alteration in the core of the type II focal cortical dysplasia. Dymorphic neurons showed increased dendritic complexity, reduction of dendritic spines and occasional filopodia-like protrusions emerging from the soma. Surprisingly, the intermingled normal-looking pyramidal neurons also showed severe spine loss and simplified dendritic arborization. No changes were observed outside the dysplasia (perilesional tissue) or in neocortical postsurgical tissue obtained in the other patient groups. Immunoreactivities of vGLUT1 and vGAT showed synaptic reorganization in the core of type II dysplasia characterized by the presence of abnormal perisomatic baskets around dymorphic neurons, in particular those with filopodia-like protrusions, and changes in vGLUT1/vGAT expression. Ultrastructural data in type II dysplasia highlighted the presence of altered neuropil engulfed by glial processes. Our data indicate that the fine morphological aspect of neurons and dendritic spines are normal in epileptogenic neocortex, with the exception of type II dysplastic lesions. The findings suggest that the mechanisms leading to this severe form of cortical malformation interfere with the normal dendritic arborization and synaptic network organization. The data argue against the concept that long-lasting epilepsy and seizure recurrence *per se* unavoidably produce a dendritic pathology.

- 1 Epilepsy Unit, Fondazione IRCCS Istituto Neurologico Carlo Besta, Milano, Italy
- 2 Department of Neurosciences, Biomedicine and Movement Sciences, University of Verona, Italy
- 3 Division of Neurology V and Neuropathology, Fondazione IRCCS, Istituto Neurologico Carlo Besta, Milano, Italy
- 4 Institute of Pathology, Department of Medical and Surgical Sciences, University of Modena and Reggio Emilia, Modena, Italy
- 5 Neurosurgery Unit, Fondazione IRCCS, Istituto Neurologico Carlo Besta, Milano, Italy
- 6 “Claudio Munari” Epilepsy Surgery Center, GOM Niguarda, Milano, Italy
- 7 Department of Pathology, GOM Niguarda, Milano, Italy

Correspondence to: Laura Rossini
Epilepsy Unit
Fondazione IRCCS Istituto Neurologico C. Besta
Via Amadeo 42, 20133 Milano, Italy
E-mail: laura.rossini@istituto-besta.it

Keywords: focal drug-resistant epilepsy; human tissue; focal cortical dysplasia; Golgi impregnation; dendritic spines

Abbreviations: FCD =focal cortical dysplasia; NN =normal-looking neuron; TLE-HS =temporal lobe epilepsy with hippocampal sclerosis

Introduction

Epilepsy is one of the most frequent neurological disorders recognized as a serious public health burden (WHO, 2017). Among the various types of epilepsies, the focal ones are of particular interest; in carefully selected difficult-to-treat focal epilepsies timely surgery is the treatment of choice (Blumcke *et al.*, 2017). Focal epilepsy is not a specific disease entity, as it includes many different aetiologies ranging from structural brain lesions (malformations of cortical development, tumours, vascular disorders), brain infections, neurodegenerative diseases and metabolic/genetic disorders. This implies that pathophysiological mechanisms may be different with respect to the different aetiologies. Moreover, in a subset of focal epilepsies defined as cryptogenic, no obvious underlying disease or neuropathologically defined lesion can be identified.

One of the key points for the prognosis and the therapy of focal epilepsies is the definition and the identification of the so-called epileptogenic zone, identified as the site of onset and primary organization of the epileptic discharges associated with seizures (Jehi, 2018). Although the epileptogenic zone is defined on an electroclinical basis, its translation into neuroanatomical details is particularly relevant when a surgical perspective is considered. The study of the neuropathological aspect of the epileptogenic zone is of fundamental interest to analyse the intrinsic organization of the epileptogenic network and to derive relevant information to understand both the pathophysiology of epilepsies and the mechanisms of epileptogenesis.

It is generally assumed that seizures derive from an imbalance between excitatory and inhibitory activity in an excessively synchronous neuronal network; however, the intimate mechanisms and the organization at the epileptogenic focus are far from being fully understood and subtle mechanisms affecting neuronal structure and function may be present.

Neuronal dendritic arborization and dendritic spines that represent the morphological sites of the majority of excitatory synaptic inputs could be critically involved in the pathophysiology of epilepsy. In fact, changes in distribution and number of dendritic spines have been suggested to be directly involved in seizures and epileptogenesis (Swann *et al.*, 2000).

In addition to the extensive literature on animal models (Wong and Guo, 2013), the presence of dendritic pathology

and spine alterations has also been reported in human tissue. Neuropathological investigations performed on patients with epilepsy associated with a genetically determined neurological disorder, such as Rett syndrome, tuberous sclerosis, Fragile X and Down syndromes (Huttenlocher and Heydemann, 1984; Machado-Salas, 1984; Hinton *et al.*, 1991; Wisniewski *et al.*, 1991; Belichenko *et al.*, 1994; Belichenko and Dahlstrom, 1995; Chappleau *et al.*, 2009; Xu *et al.*, 2014; Torres *et al.*, 2018) demonstrated dendritic pathology; in these patients it is not known whether these changes are primarily related to the genetic defect or are caused by epilepsy. In patients with seizures as the cardinal symptom, such as in epilepsies associated with either hippocampal sclerosis, or tumours, or microdysgenesis (Multani *et al.*, 1994; Belichenko and Dahlstrom, 1995; von Campe *et al.*, 1997; Blumcke *et al.*, 1999; Freiman *et al.*, 2011), neuropathological investigation revealed dendritic alterations and spine loss. However, it has not yet been determined if these alterations are the cause or the consequence of epilepsy (Fiala *et al.*, 2002; Wong and Guo, 2013).

We analysed postsurgical neocortical specimens obtained from drug-resistant epileptic patients, to investigate dendritic and spine organization as substrates of synaptic circuitries in both cortical malformations (focal cortical dysplasias, FCD) and non-malformed cases. Data were compared with autaptic neocortical samples obtained from subjects with no record of epilepsy. Based on neuronal reconstructions with Golgi technique, immunohistochemistry and electron microscopy, we demonstrate that dendritic and synaptic alterations are consistently observed in type II FCD lesions, but not in type Ia FCD or in non-malformed cases. This suggests that epilepsy *per se* does not determine structural alterations even in patients with a long-lasting history of epilepsy and high seizure frequency.

Materials and methods

Subjects and clinical work-up

The study includes the analysis of postsurgical neocortical areas from 28 subjects admitted to neurosurgery for drug-resistant epilepsy at both the Fondazione Istituto Neurologico Carlo Besta and the Claudio Munari Epilepsy Surgery Center at Niguarda Hospital (Milan, Italy). The ethics committees of both Institutes approved the diagnostic and therapeutic procedures

and the use of brain surgical specimens for research. Presurgical, surgical, and neuropathological procedures at the two centres were identical, according to the published guidelines approved by the Lombardy Region Welfare Directorate (Decreto n°1865, 15.03.2016).

All patients underwent surgery after the identification of the epileptogenic zone by electroclinical data and MRI evaluation. In seven patients, invasive presurgical stereo-EEG monitoring was performed and intraoperative interictal electrocorticography (ECoG) was carried out in six patients to identify the boundaries of the epileptogenic cortex. *En bloc* resections were performed for therapeutic reasons after the patients had given informed consent and the extent of the excision was planned preoperatively to minimize risks of postsurgical deficits on the basis of the epileptogenic zone location. Seizure outcome was assessed according to the Engel classification (Engel *et al.*, 1993) at least 2 years after surgery, unless otherwise indicated.

The neuropathological diagnosis was FCD in 18 patients: type Ia ($n = 1$) was characterized by mild abnormal cortical layering and persistent radial microcolumnar architecture; type II presented severe disorganization and the presence of dysmorphic neurons (IIa, $n = 5$) and balloon cells (IIb, $n = 12$). The non-malformed cases were cryptogenic (no lesion, $n = 5$) and patients with temporal lobe epilepsy due to hippocampal sclerosis (TLE-HS, $n = 5$) without obvious MRI or histological alterations in the temporal neocortex. Non-epileptic control tissue was obtained from autopsies performed within 48 h after death in two adult subjects without history of seizures or neurological diseases; the tissue was obtained and processed in agreement with the Declaration of Helsinki. Table 1 summarizes the patient data.

Morphological procedures

After surgery, *en bloc* resected brain specimens were immediately immersed in fixative solution (4% paraformaldehyde) for 24 to 36 h. Blocks were cut in 5-mm thick slabs that were paraffin embedded or cut using a vibratome (VT1000S; Leica). In a subgroup of 13 cases (five FCD IIb, three FCD IIa, one FCD Ia, two cryptogenic, two TLE-HS), according to tissue availability, a 3-mm thick slab was cut from the fresh specimen in the surgery theatre immediately after the resection and was immersed in an appropriate solution for Golgi-Cox impregnation, as described below. In MRI-positive cases, the slab was cut according to imaging data to include part of the lesion; in MRI-negative cases, the slab was chosen where the most epileptogenic activity was identified by the stereo-EEG in one case or in the middle of the resected specimen in the other. In autopsic cases, tissue blocks from cortical brain regions were sampled for Golgi-Cox impregnation and for adjacent neuropathological control.

Golgi-Cox impregnation

A modified Golgi-Cox protocol was used according to Zaqout and Kaindl (2016). The slabs were immersed for 10 days in the Golgi-Cox solution (Glaser and Van der Loos, 1981) composed of a mixture of 5% potassium dichromate ($K_2Cr_2O_7$), 5% potassium chromate (K_2CrO_4) and 5% mercury chloride ($HgCl_2$) in distilled water. After rinsing in 30% sucrose solution for 24 h, the tissue was embedded in agar (6%) and cut in 200- μ m thick sections collected in a 6% sucrose solution. After rapid

rinses in distilled water, the sections were incubated for 15 min in a solution of ammonium hydroxide (NH_4OH), rinsed in distilled water and immersed for 15 min in 1% solution of sodium thiosulphate ($Na_2S_2O_3$). Sections were then repeatedly washed in distilled water, dehydrated in graded alcohols, cleared in a solution of one-third chloroform, one-third xylene, one-third alcohol for 15 min and mounted with DPX (BDH Lab Supplies).

Dendritic tree complexity and spine density analysis

The quantitative evaluation of dendritic arborization and spine density was performed in selected patients, as indicated in Table 1. For dendritic branching, the Golgi-impregnated neocortical neurons were analysed at $\times 40$ with a Nikon Eclipse E1000M microscope equipped with a motorized stage interfaced to a computer. To select the neurons for the 3D reconstruction, the following criteria were used: full impregnation with no apparent basal and apical dendritic truncation; characteristic triangular soma shape for normal pyramidal neurons; irregular morphology and soma size $> 25 \mu$ m in diameter for dysmorphic neurons; and presence of dendritic spines. A total of 10 pyramidal neurons, five in superficial and five in deep layers, from each sample were fully 3D reconstructed in autopsy, cryptogenic, TLE-HS and type Ia FCD cases. In TLE-HS the temporal neocortex was analysed. In type II FCD tissue, from each sample we reconstructed 10 dysmorphic neurons and 10 normal-looking pyramidal neurons (NNs) in the core of the lesion, and 10 NNs in the adjacent perilesional tissue (identified by the absence of dysmorphic neurons). The 3D reconstruction of impregnate neurons was performed using a dedicated software (Image-Pro Plus 7.0, Media Cybernetics, Silver Spring, MD). To improve the quality of images, AutoquantX 3.1 software was used for image deconvolution (Media Cybernetics, Rockville, MD). Images were then imported into the Imaris x6.4 9.1.2 software (Bitplane AG Scientific Solutions, Zurich) for reconstruction. The following three parameters were quantified: (i) filament area, considered as the area occupied by all dendrite segments; (ii) dendritic branching points; and (iii) dendritic tree complexity with Sholl analysis, which measures the number of dendrites crossing circles at various radial distances from the cell soma (Sholl *et al.*, 1953). See Supplementary Fig. 1 for further details.

For spine density, two acquisitions on apical and two on basal dendrites were performed at higher magnification ($\times 60$) in neurons similar to those considered for dendritic arborization. These acquisitions were centred at the same distance from the soma, and covered the entire dendritic tree in NNs, but not in dysmorphic neurons because of their large size. The dendritic spine number along dendritic branches was manually evaluated using the ImageJ software (<http://imagej.nih.gov/ij/>); spine density was calculated as the ratio between the number of spines and the length of the dendritic segment.

For each of these parameters, differences among groups were statistically evaluated using one-way ANOVA followed by Bonferroni *post hoc* comparison test using Origin Pro 2018b (Northampton, MA, USA). Data are expressed as mean \pm standard deviation (SD).

Table 1 Clinical data of the patients

ID	Diagnosis	Age at epilepsy onset, years	Epilepsy duration, years	Age at surgery, years	Monthly seizure frequency	Invasive recording	Site of surgery	Outcome (Engel class)	Golgi
1	FCDIA	9	4	13	8	SEEG	T	IA ^a	Quant.
2	FCD IIB	3	49	52	12	EcoG	F	IC	Quant.
3	FCD IIB	7	15	22	15	No	F	IA	Quant.
4	FCD IIB	11	18	29	60	EcoG	F	IA ^a	Quant.
5	FCD IIB	12	12	24	12	No	TO	IA	Qual.
6	FCD IIB	9	33	42	4	No	F	IA	Qual.
7	FCD IIB	1	5	6	3	No	O	IA	
8	FCD IIB	1	33	34	16	EcoG	F	IA	
9	FCD IIB	4	27	31	90	EcoG	F	IA	
10	FCD IIB	13	13	26	90	EcoG	FC	II	
11	FCD IIB	1	1	2	90	EcoG	F	IA	
12	FCD IIB	6	40	46	75	EcoG	P	IA	
13	FCD IIB	0	5	5	500	No	O	IA	
14	FCD IIA	0	6	6	0.5	SEEG	T	IA ^a	Quant.
15	FCD IIA	4	6	9	0	No	F	IA ^a	Quant.
16	FCD IIA	0	6	6	200	SEEG	O	IA	
17	FCD IIA	1	15	16	10	No	F	III	Qual.
18	FCD IIA	0	1	1	300	No	TO	IA	
	Mean	4.3	16.8	21.0	86.9				
	SD	4.6	14.4	16.0	125.9				
19	Crypto	29	17	46	40	No	T	IA ^a	Quant.
20	Crypto	8	27	35	10	SEEG	T	IA ^a	Quant.
21	Crypto	19	25	44	20	SEEG	F	IC ^a	
22	Crypto	16	14	30	5	SEEG	T	IA	
23	Crypto	39	4	43	3	SEEG	T	III	
	Mean	22.2	17.4	39.6	15.6				
	SD	12.0	9.2	6.8	15.1				
24	TLE-HS	7	28	35	2	No	T	IA	Quant.
25	TLE-HS	10	30	40	20	No	T	IA	Quant.
26	TLE-HS	18	20	38	1	No	T	IA	
27	TLE-HS	6	44	50	5	No	T	IA	
28	TLE-HS	19	15	34	4	No	T	ID	
	Mean	12.0	27.4	39.4	6.4				
	SD	6.1	11.1	6.4	7.8				
29	Autopsy			80			T		Quant.
30	Autopsy			69			F		Quant.

^aPatients with a follow-up of <2 years.

C = central; crypto = cryptogenic; EcoG = electrocorticography; ID = identification number; F = frontal; O = occipital; P = parietal; Qual. = qualitative data; Quant. = quantitative data; SD = standard deviation; SEEG = stereo-EEG; T = temporal.

Neuropathological analysis

For routine neuropathology, 7- μ m thick paraffin sections were cut and stained with thionin (0.1%), haematoxylin and eosin, and Kluver-Barrera. Additional serial sections were processed for immunohistochemistry using antibodies against glial fibrillary acidic protein (GFAP, 1:1000, Millipore), non-phosphorylated neurofilaments (SMI311R, 1:250, Covance), intermediate filament protein vimentin (1:1000, Dako), neuron-specific nuclear protein (NeuN, 1:1000, Millipore), vesicular transporters of glutamate (vGLUT1, 1:500, Synaptic System) and GABA (vGAT, 1:200, Synaptic System). Single-label immunohistochemistry was developed using the avidin-biotin peroxidase method and 3,3'-diaminobenzidine (Sigma) as chromogen, as described elsewhere (Garbelli et al., 1999), on sections counterstained with haematoxylin. In two selected type II FCD cases,

50- μ m thick vibratome sections were used for double immunofluorescence labelling. The sections were incubated in a mixture of SMI311/vGLUT1 or SMI/vGAT followed by a mixture of indocarbocyanine (Cy) 2-conjugated goat anti-mouse and (Cy) 3-conjugated goat anti-rabbit antibodies. The sections were then mounted with FluorSaveTM (Millipore) and observed using a confocal microscope (TCS-SP5 Leica Microsystem).

Quantitative analysis of presynaptic markers

Quantification of vGLUT1 and vGAT presynaptic markers in type II FCD cases was performed on single labelled sections. Briefly, in one section per case two regions of interest in the grey matter were acquired at 40 \times of magnification, with a Nikon digital camera, in the region of lesion and in the adjacent

perilesional area. The total considered area was 0.088 mm². After quenching haematoxylin signal and grey conversion using the Image-Pro Premier 9.1 software, the optical density (the mean grey value among the pixels in the region of interest) was measured using ImageJ software. Changes between lesional and perilesional area were then evaluated with two-sample *t*-test. Data are expressed as mean ± SD.

Transmission electron microscope

In two type IIb FCD cases, grey matter ultrastructural morphology was analysed on a vibratome section embedded for electron microscopy using a previously published protocol (Zucca *et al.*, 2016). In particular, areas of interest detected on osmicated sections corresponding to the core of the lesion and the adjacent perilesional area were excised and prepared for ultrastructural examination under a TecnaiTM Spirit TEM (FEI).

Data availability

The data that support the findings of this study are available on request from the corresponding author.

Results

Clinical features

The main clinical characteristics of the patients are summarized in Table 1. In the type II FCD group, the mean age at seizure onset was lower than in cryptogenic and TLE-HS patients, whereas the mean seizure frequency at the time of surgery was higher, in agreement with published data (Blumcke *et al.*, 2017, Rossini *et al.*, 2017). Patients with TLE-HS had an epilepsy time span longer than other groups. The majority of the considered patients were adults at the time of surgery, with the exception of the FCD II cohort, which also included paediatric patients. The postsurgical outcome was Engel class I in 25 patients (89%); in one patient, seizure outcome was Engel class II and in two patients was class III.

Dendritic pathology and spine loss

Although Golgi impregnation labels approximately one-tenth of the total cortical neuronal population, the general architecture of the cortex was recognizable. In control autoptic cases, as well as in cryptogenic and TLE-HS, where neuropathology demonstrated a normal cortical lamination, the impregnated neurons appeared regularly distributed and a six-layered cortex was visible (Fig. 1A and B). In the case of type Ia FCD, Golgi-impregnated neurons were arranged in columnar disposition (Fig. 1D), as confirmed in adjacent NeuN-stained sections (Fig. 1C): a vertical orientation of dendrites was clearly evident at low magnification and apical dendrites were aligned at higher magnification (Fig. 1G). In the perilesional area of type Ia FCD, normal cortical organization was visible in Golgi-impregnated sections (Fig. 1H). The aspect of the cortex in type II FCD cases was very

different. Within the core of the lesion, empty areas, probably due to neuronal loss (Fig. 1E), were intermingled with a dense and irregular net of thick dendrites originating from dysmorphic neurons. The cortical dendritic network appeared dramatically disarranged and dysmorphic neurons were clearly recognized by the enlarged, bizarre morphology of perikaryon (Fig. 1F and yellow arrows in Fig. 1I). Small neurons with a normal-looking morphology were also identified, intermingled with dysmorphic neurons (red arrows in Fig. 1I). In type IIb FCD, vimentin-positive balloon cells (Fig. 1J) were also impregnated and identified by their large cell bodies and enormous branching of processes (Fig. 1K). In the adjacent perilesional areas of both FCD IIa and IIb, normal cortical organization was observed (data not shown).

Cell morphology was analysed in detail at higher magnification (Fig. 2A–D) and using 3D reconstruction (Fig. 2A'–D'). In control autoptic tissue as well as in cryptogenic, TLE-HS, type Ia FCD and type II FCD perilesional areas, pyramidal spiny neurons had normal morphology with regularly oriented apical dendrites and recognizable basal dendrites. The proximal apical dendrites had few collaterals and branching increased toward layer I; the basal dendrites were clearly visible with numerous branching covering a wide area around the neuron. Axons emerging from the base of the soma with recognizable axon hillock were identified and reconstructed only at short distance from the soma; this is an intrinsic limitation of the Golgi method performed in specimens from adult subjects. Next, we quantified dendritic area, branch points and dendritic complexity with Sholl intersection analysis in fully reconstructed pyramidal neurons; in agreement with the qualitative evaluation, no significant differences of these parameters were observed among groups, except for a reduction of branch points in TLE-HS versus autopsy (Fig. 3A–C and Supplementary Table 1).

By contrast, in the core of type II FCD dendritic abnormalities were present in both dysmorphic neurons and NNs. Increased dendritic number and thickness with a complete disruption of the normal apical and basal organization were typically observed in dysmorphic neurons (Fig. 2F, F', H and H'). The soma was enlarged with abnormal morphology; in a few cases large neurons with a pyramidal morphology were still visible (Supplementary Fig. 2). Surprisingly, NNs exhibited a dramatic simplification of dendritic branching complexity; although the apical and basal dendrites were still recognizable, they showed reduced arborization (Fig. 2E, E', G and G') and appeared thinner in comparison with normal pyramidal neurons observed both in the adjacent perilesional tissue and in autoptic cases. The quantification of the three parameters revealed that branch points and dendritic complexity were higher in dysmorphic neurons and lower in NNs, respectively in both type IIb/IIa FCD core regions compared to autopsy controls while the area occupied by all dendrite segments was significantly altered in dysmorphic neurons in type IIb FCD and in NNs in type IIa (Fig. 3D–F and Supplementary Table 1). Differences between

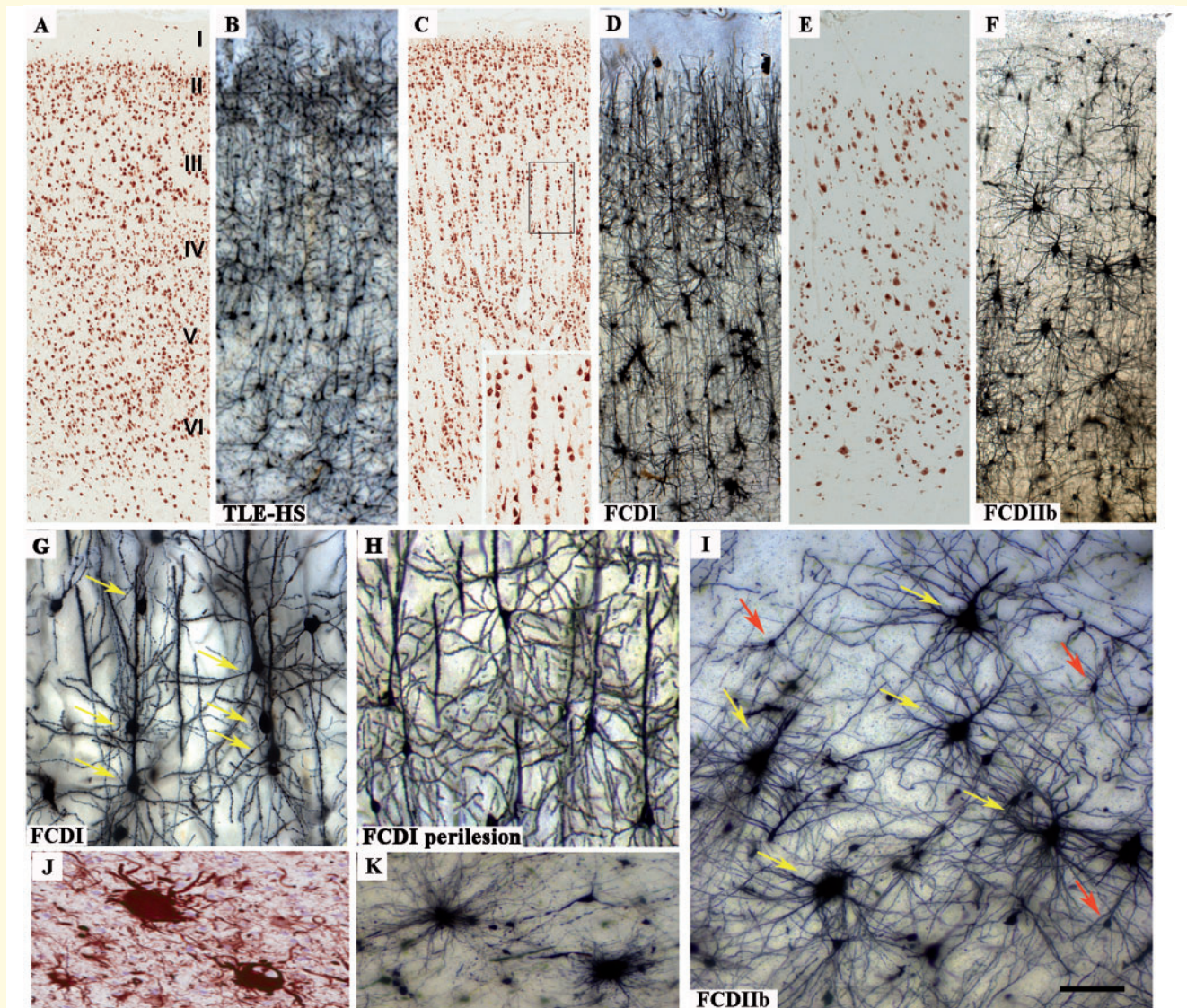


Figure 1 Architectural and cytoarchitectural features in Golgi-impregnated sections. (A–F) Low power microphotographs of Golgi-impregnated and NeuN-stained adjacent sections showing a normal cortical architecture with recognizable cortical layers in the temporal neocortex in a TLE-HS case (A and B), radial columnar organization of the neurons in type Ia FCD (C and D), and severe cortical disorganization with reduced neuronal density in type IIb (E and F). (G and H) Details showing the vertical alignment of neurons (G, yellow arrows), a hallmark of type Ia FCD, that is not present in the adjacent perilesional region (H). (I) In type IIb FCD, giant dysmorphic neurons (yellow arrows) with increased and disorganized dendritic tree are intermingled with small pyramidal neurons showing apparent normal morphology (NNs, red arrows), but a simplified dendritic arbor. (J and K) Examples of balloon cells in vimentin-stained and Golgi-impregnated sections, respectively. Scale bar represents: 370 μm (A–F), 60 μm (G and H), 130 μm (J–I).

type IIb/IIa FCD cases are summarized in a [Supplementary Table 2](#). In a subpopulation of dysmorphic neurons, numerous, short filopodia-like protrusions that emerge from the soma were observed in both Golgi-impregnated sections and in thick sections immunoreacted for neurofilaments (Fig. 4).

In cryptogenic, TLE-HS and type Ia FCD cases and in perilesional tissue of type II FCD, dendritic spine morphology and distribution were similar to control autaptic tissue (Fig. 5A–E). Conversely, in dysmorphic neurons and NNs in the core of the type II FCD lesion, several abnormalities

were present, such as alterations/distortions in spine shapes, irregular distributions and presence of dendritic varicosities (Fig. 5F–K). Spine density was significantly decreased in both dysmorphic neurons and NNs in type IIb FCD lesion, while in type IIa the reduction was less severe and statistically significant only for NNs; no differences were found among the other groups (Fig. 6A and B, [Supplementary Tables 1 and 2](#)). When the dendritic spine density, referred to each neuronal element (dysmorphic neurons and NNs in type II FCD and control neurons in autopsy) was plotted

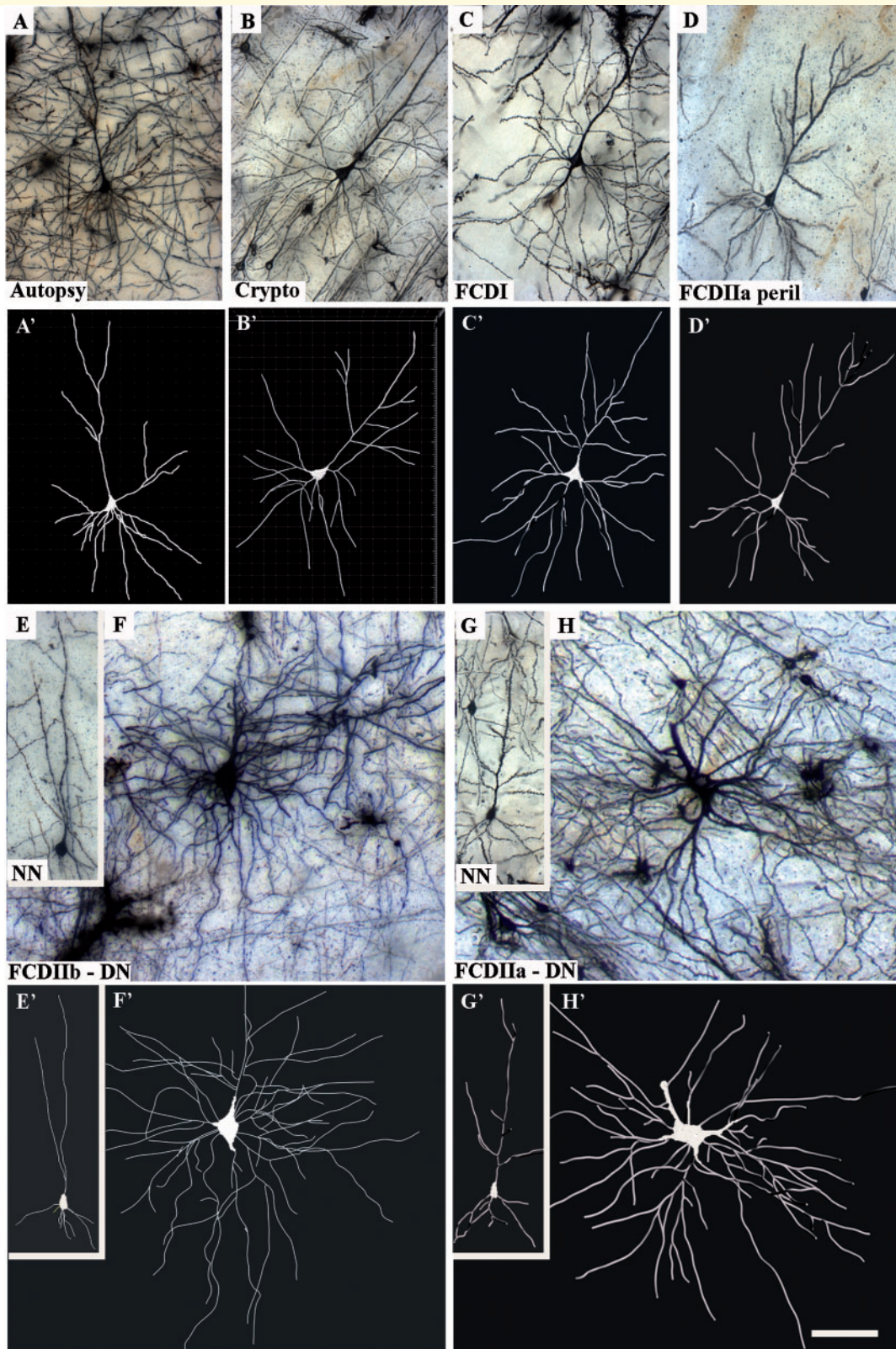


Figure 2 Three-dimensional reconstructions of dendritic morphology. High power microphotographs of Golgi-impregnated pyramidal neurons (**A–H**) and corresponding 3D reconstructions (**A'–H'**). (**A–D** and **A'–D'**) Note the presence of a similar dendritic arborization with well-defined apical and basal domains in control autopsy, crypto, type Ia FCD, and perilesion of type II FCD. (**E–H** and **E'–H'**) Note the dramatic reduction of dendritic arbors in both apical and basal domains in NNs in the core of the type II FCD. Dysmorphic neurons (DN) show increased soma size and apical dendrite thickness, coupled with large dendritic complexity. Scale bar represents: 115 μm (**A–H**).

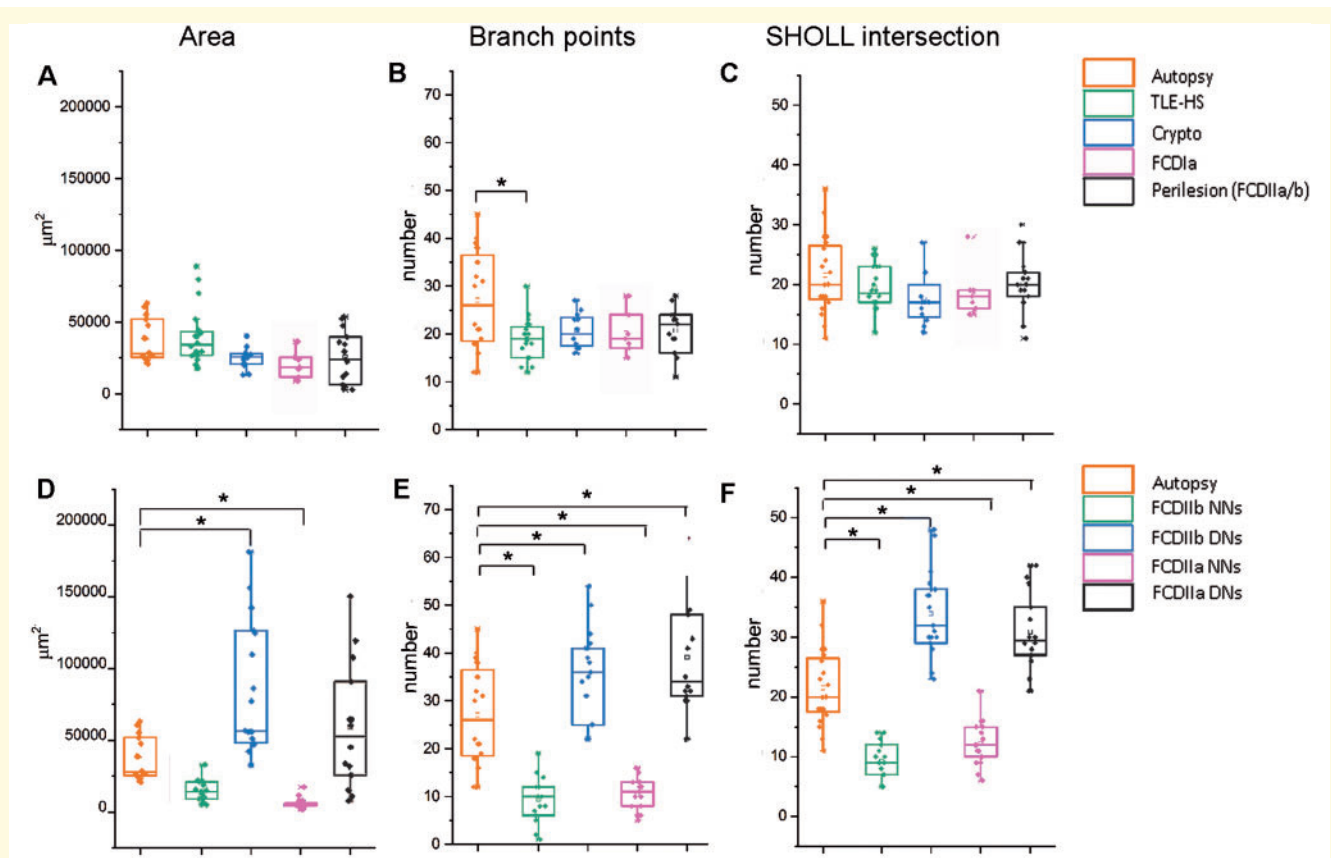


Figure 3 Quantification of dendritic complexity. (A–F) Box plots showing the evaluation of the dendritic parameters measured on Golgi-reconstructed neurons in the different patient groups. Quantitative measurements confirm the significant decrease in dendritic complexity in NNs and the significant increase in dysmorphic neurons from type II FCD in comparison with control autopsy. No differences were observed among control autoptic cases, TLE-HS, cryptogenic, type Ia FCD and perilesional FCD II tissue, except for branch points. Asterisks indicate statistical significance (* $P < 0.05$).

from the highest to the lowest value, the remarkable reduction occurring in NNs and dysmorphic neurons compared to autopsy was very clear and the lowest values were obtained in neurons from type IIb FCD cases (Fig. 6C, red and light blue colours for type IIb and blue and yellow for type IIa).

Synaptic abnormalities

The dendritic and spine abnormalities within the core of the type II FCD, prompted us to analyse synaptic inputs. We evaluated synaptic excitatory and inhibitory input to soma and dendrites of neurons by immunohistochemistry and confocal immunofluorescence in sections reacted with specific glutamatergic (vGLUT1) and GABAergic (vGAT) presynaptic markers. In type II FCD perilesion tissue, as well as in cortical specimens of type Ia FCD, of cryptogenic and of TLE-HS, both vGLUT1 and vGAT immunoreactivities were present in all layers and were associated with fine punctate structures homogeneously distributed around unlabelled soma and proximal processes (Fig. 7A and C). Vertical rows of immunoreactive puncta, interpreted as axon initial

segments, were evident with vGAT staining (Fig. 7C). By contrast, in the core of the FCD lesion the immunoreactive puncta were more dispersed and were particularly concentrated around the perikaryal profile of some dysmorphic neurons (Fig. 7B and D). This abnormal perisomatic synaptic labelling was confirmed in both type IIa and IIb FCD by double immunofluorescence combining SMI311 with vGLUT1 and vGAT. Perisomatic baskets were particularly evident around dysmorphic neurons presenting filopodia-like protrusions (Fig. 7E–H). The quantification of the synaptic markers showed reduced vGLUT1 and increased vGAT immunoreactivities in type IIb FCD lesions compared to the adjacent perilesional tissue; no significant differences were observed in type IIa (Fig. 7I). These data suggest an overall reorganization of excitatory and inhibitory input within type II FCDs.

In two representative type IIb FCD cases, we performed ultrastructural analysis of the grey matter in the core of the lesion and in the adjacent perilesional area. In the lesion, the neuropil was almost entirely occupied by profiles exclusively containing bundles of intermediate filaments; it was extremely rare to observe synaptic terminals. By contrast, in the

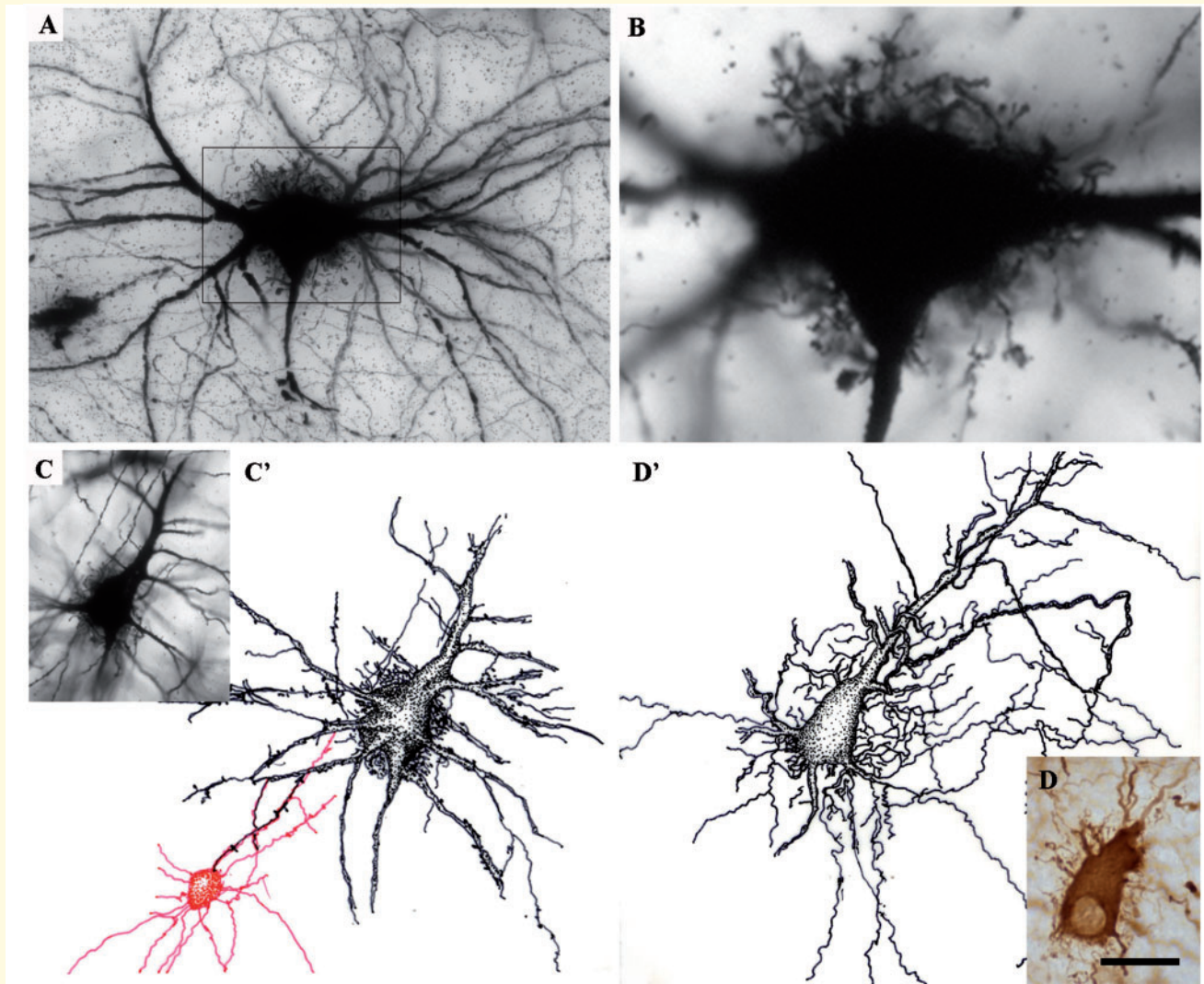


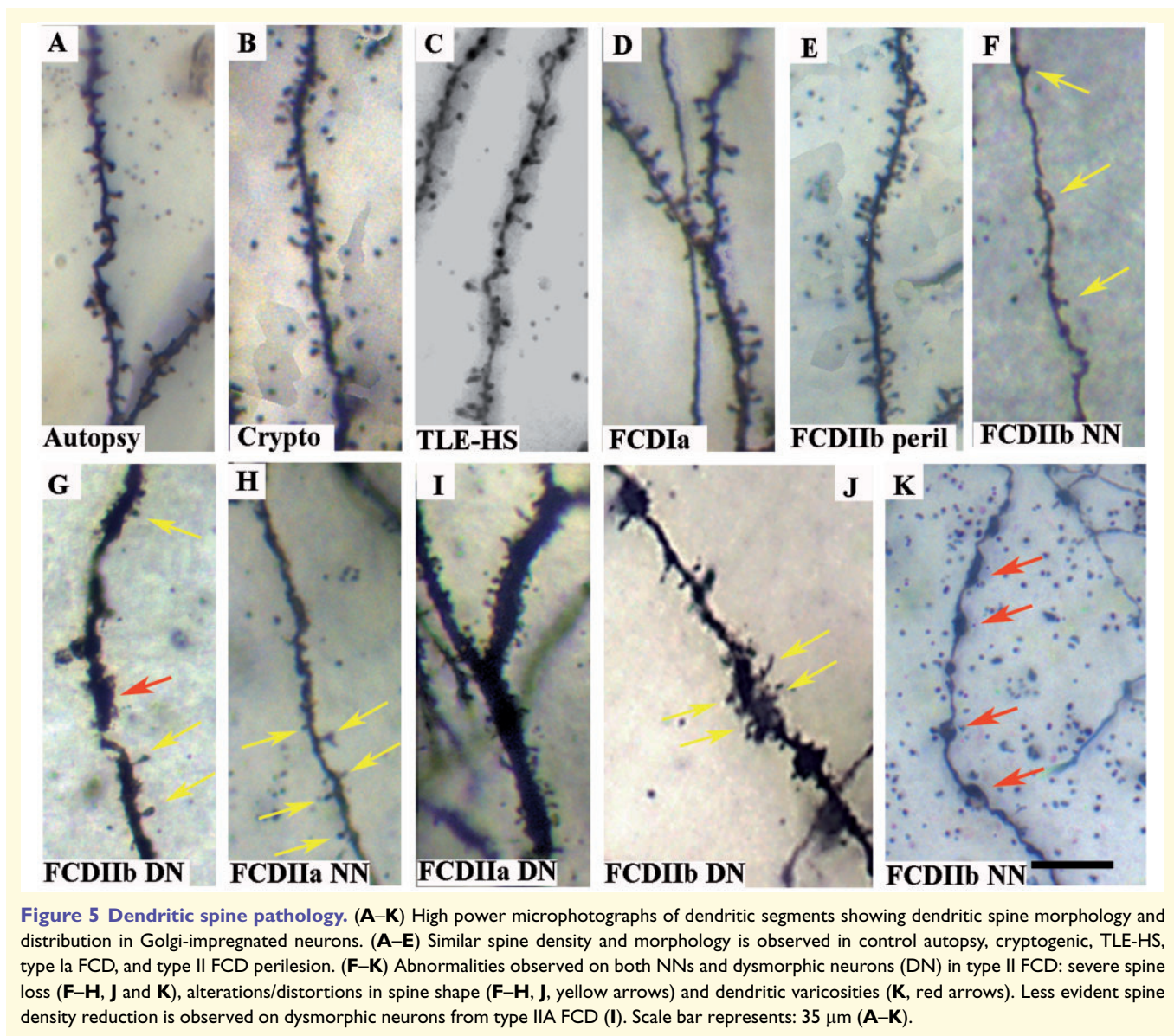
Figure 4 Filopodia-like protrusions in dysmorphic neurons. (A and B) Low and high power microphotographs of Golgi-impregnated dysmorphic neuron from a type IIb FCD showing the presence of numerous short filopodia-like protrusions emerging from the soma. (C and D) Other examples of dysmorphic neurons with filopodia-like protrusions visible on Golgi-impregnated section (C) and neurofilament-stained section (D). (C' and D') Camera-lucida drawing of the dysmorphic neurons showed in C and D, respectively. In C' a non-spiny interneuron close to the dysmorphic neuron is also drawn in red. Scale bar represents: 35 μm (A); 12 μm (B); 45 μm (C and D).

perilesion we observed normal ultrastructural features, and the presence of axon terminals forming synapses on different neuronal profiles (Fig. 7J and K).

Discussion

In a recent paper we demonstrated that markers of tissue damage, such as neuronal loss, extended gliosis and the presence of inflammatory signs were detected in the lesional area of type II FCD, particularly in the subtype IIb, but not in adjacent perilesional and in cryptogenic tissue (Rossini *et al.*, 2017). We have now extended the morphological analysis to subtle neuronal structures, revealing that severe dendritic and spine alterations occur in both dysmorphic neurons and

NNs in the core of the FCD type II lesion. Presynaptic excitatory and inhibitory inputs are also rearranged. The adjacent perilesional area in FCD II cases shows dendrite and spine structure similar to control autoptic tissues, and the same was also found in the neocortex of both cryptogenic cases and a type Ia FCD patient and in the temporal neocortex of patients with TLE-HS. These data suggest that the pathogenic mechanisms leading to the severely epileptogenic type II FCD not only produce the well-known cytological alterations (Blümcke *et al.*, 2011), but also change the fine morphology of dendrites and spines and alter the distribution of synaptic membrane molecules. A relevant conclusion of our study is the confirmation that in patients with a long history of seizure recurrence, such as cryptogenic, TLE-HS and FCD type Ia cases, the neocortex is structurally



preserved for the analysed parameters, suggesting that seizure activity *per se* does not produce dendritic/spine pathology.

Although a wide variety of dendritic protrusions have been described in the brain, simple dendritic spines constitute the postsynaptic site for most of the excitatory synapses on pyramidal neurons (Fiala and Harris, 1999). The spine density is directly related to the degree of neuronal connectivity (Spruston, 2008) and pathological changes in spine distribution have been related to a wide variety of neurological disorders, including epilepsy.

Studies on human epileptic tissues and animal models of epilepsy have reported dendritic spine loss and the occurrence of varicose swellings of dendritic branches: these changes were proposed to be the consequence of seizure-induced neuronal damage (Swann et al., 2000; Wong, 2005). However, these studies do not exclude the possibility

that the initial epileptogenic insults might have a primary impact on the observed dendritic abnormalities. The majority of data on human epileptic tissues were derived from patients with TLE-HS and were focused on pyramidal neuron and dentate granule cell abnormalities in the sclerotic hippocampi (Scheibel et al., 1974; Isokawa and Levesque, 1991; Isokawa, 1997; Isokawa et al., 1997; von Campe et al., 1997; Blumcke et al., 1999; Freiman et al., 2011). It is well established that TLE-HS is the result of an initial precipitating injury that is able to produce long-lasting alterations of the hippocampal structure, such as pyramidal cell loss, sprouting of the mossy fibres and gliosis, a set of alterations similar to those found in type II FCD lesions. On the contrary, few studies have previously analysed the presence of dendritic pathology in neocortical epileptic tissues. Multani et al. (1994), using Golgi-impregnated neurons, found alterations of dendritic branching and reduction of

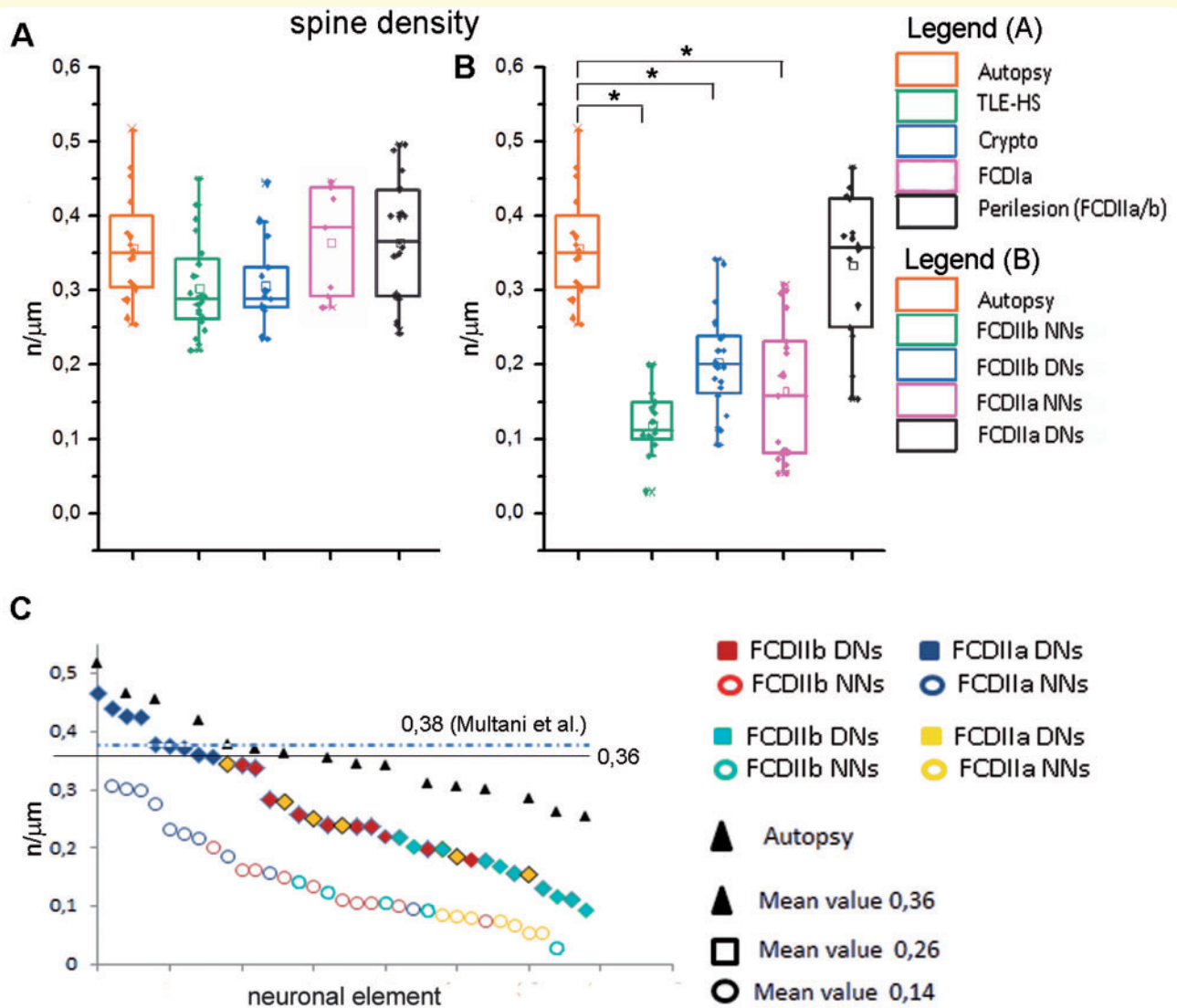


Figure 6 Quantification of spine loss. (A and B) Box plots confirming the significant reduction of spine density in both NNs and dysmorphic neurons (DN) in type IIb FCD in comparison to control autopsy samples; in type IIa the reduction is significant only for NNs. No differences were observed among control autopsic cases, type Ia FCD, TLE-HS, cryptogenic and type II FCD perilesions. Asterisks indicate statistical significance ($*P < 0.05$). (C) Graphic representing the spine density referred to each neuronal element ordered on the x-axis from the highest to the lowest value. Squares for dysmorphic neurons (DNs) and circles for NNs in type II FCD, triangles for normal neurons in autopsy. Each colour represents a different case (light blue and red for type IIb FCD, yellow and blue for type IIa FCD, black for autopsy). The black line is the average spine density obtained in our autopsic cases (0.36) compared to that published by [Multani et al. \(1994\)](#) (blue dashed line, 0.38). Note the severe spine loss occurring in both NNs and dysmorphic neurons in comparison to autopsy, more pronounced in neurons from type IIb cases.

spine density in neocortical tissues from patients with no specific lesion, hippocampal sclerosis and tumours. These data are different from our results on cryptogenic cases although our results for spine density in control autopsic tissues were similar. [Vaquero et al. \(1982\)](#) reported no alteration in spine density in pyramidal neurons from frontal and temporal neocortices of epilepsy patients, not further specified, while [Belichenko and Dahlstrom \(1995\)](#), using Lucifer yellow microinjections and confocal microscopy, observed reduced dendritic spines in cortical neurons from patients with Rett syndrome and in ‘microdysgenetic’ cortex,

but not in the adjacent regions. Interestingly, microdysgenesis was used to describe several forms of cortical alterations now included in the spectrum of FCDs ([Kasper et al., 1999](#)).

A novel finding of the present study is the presence of quantified dendritic alterations and spine loss on dysmorphic neurons in type II FCD postsurgical tissues. This is not an unexpected finding, since it has recently been demonstrated that these abnormal cells may arise from somatic mutations in genes encoding regulatory proteins of the mTOR signalling cascade occurring in progenitor cells during development ([D’Gama et al., 2017](#); [Marsan and Baulac, 2018](#);

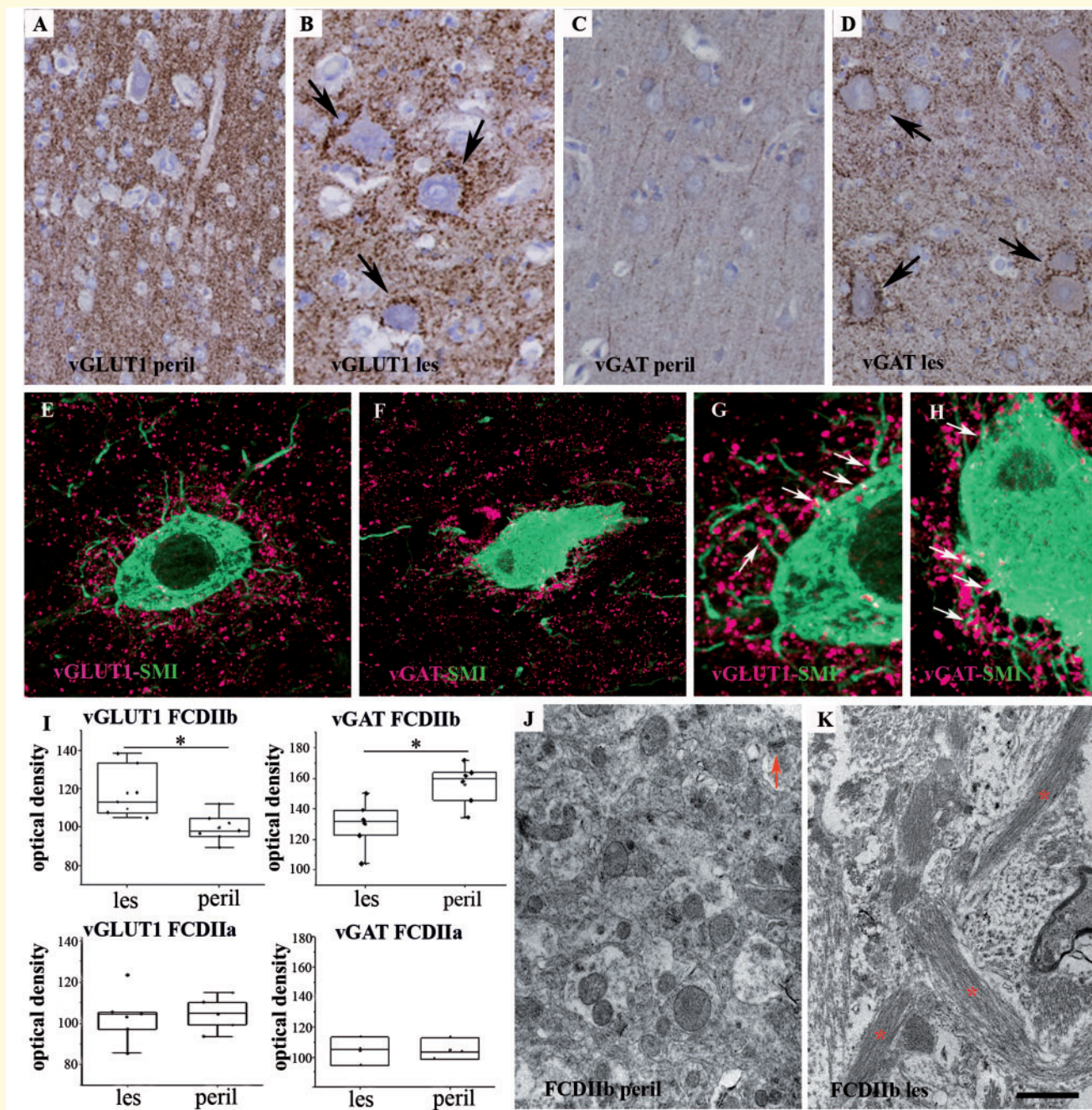


Figure 7 Synaptic abnormalities in type II FCD. (A–D) Examples of vGLUT1 and vGAT immunoreactivities in type II FCD. Note the different distribution in perilesions (peril) compared to the core of the dysplasia and the presence of basket formations around dysmorphic neurons (DNs, arrows) with both synaptic markers. (E–H) Confocal images confirming the presence of perisomatic excitatory vGLUT1 (E and G) and inhibitory vGAT-positive axons terminals (F and H) around dysmorphic neurons presenting filopodia-like protrusions (indicated by white arrows in G and H). (I) Quantification of the synaptic markers showing increased vGLUT1 optical density (corresponding to a reduction of immunoreactivity) and decreased vGAT optical density (corresponding to an increase of immunoreactivity) in type IIb lesions (les) compared to adjacent perilesions; no significant differences are observed in type IIa FCD. (J and K) Electron micrographs comparing the appearance of the neuropil in the perilesional area (J) versus the core of the lesion (K); note the presence of numerous profiles containing bundles of intermediate filaments (asterisks) that engulfed the neuropil in the lesion and the lack of synaptic contacts that are visible in the perilesion (arrow). Scale bars represents 45 μ m (A–D); 25 μ m (E and F); 12.5 μ m (G and H); 1 μ m (J); 2 μ m (K).

Baldassari *et al.*, 2019; Ying *et al.*, 2019). The identified mutations induce hyperactivation of the mTOR pathway with consequences on several important functions, such as cell growth, proliferation and survival, dendrite branching and spine shaping (Crino, 2011). Moreover, mTOR inhibitors affect dendritic arbour development (Jaworski and Sheng, 2006). Finally, spine density is low both in patients with tuberous sclerosis, a genetic disease associated with mTOR pathway hyperactivation due to *TSC1* and *TSC2* gene mutations, and in experimentally induced loss of *TSC1* and *TSC2* genes in cultured neurons (Machado-Salas, 1984; Tavazoie *et al.*, 2005).

Based on these data, we hypothesize that the presence of a hyperactivated mTOR pathway, proven with pS6 immunoreactivity in our type II FCD cases, may trigger structural changes in dendrites and spines of dysmorphic neurons. We do not prove the presence of somatic variants in our cases, notwithstanding, the current literature suggests that in spite of the presence of mTOR hyperactivation, in many patients it is not possible to detect causative or putative mutations, probably due to brain mosaicism below the detection level (Marsan and Baulac, 2018; Sim *et al.*, 2019).

Unexpectedly, we found important morphological alterations on NNs in the core of the FCD lesion, characterized by a dramatic reduction in dendritic tree and severe spine loss, although these neurons are not supposed to carry somatic mutations (Baldassari *et al.*, 2019). We can speculate that mutated cells (i.e. dysmorphic neurons and balloon cells) with their altered activity may induce secondary changes on surrounding normal neurons through release of growth factors or neurotransmitters (LaSarge and Danzer, 2014; Iffland and Crino, 2019).

In some Golgi-impregnated dysmorphic neurons we observed the presence of numerous short filopodia-like protrusions emerging from the soma. During development, and particularly during synaptogenesis, long and thin protrusions emerge from the soma, dendrites and axons; these filopodia are highly motile structures likely involved in the process of synaptogenesis (Fiala *et al.*, 2002). They are not seen on mature neurons and their presence on dysmorphic neurons may be a sign of immaturity. We do not know whether the dysmorphic neuron protrusions are proper filopodia, as seen during early developmental stages, or malformed dendritic processes. These protrusions were frequently coupled with the presence of abnormal hypertrophic basket of vGLUT1 and vGAT-immunoreactive puncta that were never observed in the adjacent perilesional area.

Interestingly, some of the morphological alterations we report on Golgi-impregnated neurons were previously observed in biocytin-filled cells derived from different forms of cortical malformations in paediatric patients (Cepeda *et al.*, 2003). The authors described varicose and tortuous dendrites on cytomegalic neurons and the presence of a simplified dendritic tree on immature cells coupled with abnormal intrinsic membrane properties. Our data, obtained on adult cases, imply that the observed alterations are not related to the age of the patients.

The presence of GABAergic sprouting on dysmorphic neurons has already been reported and was suggested to sustain postsynaptic hyperexcitability (Garbelli *et al.*, 1999; Ellender *et al.*, 2014; Medici *et al.*, 2016). The demonstration of glutamatergic baskets on dysmorphic neurons, associated with the reduction of spine density along the dendrites and neuropil engulfed of intermediate filaments, suggest the presence of synaptic reorganization in neuronal circuitry within the FCD lesion. We propose that excitatory terminals fail to find appropriate postsynaptic sites along the dendrites, and form abnormal synapses on dysmorphic neuron soma and/or filopodia-like protrusions. Interestingly, the integration of excitatory inputs is greatly influenced by their location on dendrites; excitatory synapses on the soma and in its proximity, as suggested by the presence of perisomatic glutamatergic basket formations, are expected to facilitate action-potential initiation (Spruston, 2008), thus promoting hyperexcitability.

The less severe alterations we found in type IIa compared to type IIb FCD, in terms of spine density on dysmorphic neurons and quantitative alterations on synaptic markers may be biased by the low number of cases that we had the opportunity to study. Further studies with a larger cohort are required to define possible intrinsic differences between the two subtypes.

In conclusion, the present data show severe rearrangement of both neuronal morphology and synaptic networks in the core of the type II FCD (particularly type IIb), but not in the surrounding perilesional tissue. The study also demonstrates that, except for type II FCDs, neurons and dendritic spines are structurally normal in highly epileptogenic neocortices. These findings substantiate the hypothesis that seizures *per se* do not promote structural alteration of the neocortex even in patients with a longstanding history of epilepsy and high seizure rate.

Acknowledgements

We would like to acknowledge Dr Barbara Cipelletti for technical assistance.

Funding

The study was supported by the Italian Ministry of Health grant RF-2016-02362195 (to R.G.), AICE-FIRE Foundation RA-101 (to L.R.), NET-2013-02355313 and EpiCARE 2017-2020 by Associazione Paolo Zorzi per le Neuroscienze.

Competing interests

The authors report no competing interests.

Supplementary material

Supplementary material is available at *Brain* online.

References

- Baldassari S, Ribierre T, Marsan E, Adle-Biassette H, Ferrand-Sorbets S, Bulteau C. Dissecting the genetic basis of focal cortical dysplasia: a large cohort study. (Review). *Acta Neuropathol* 2019; 138: 885–900.
- Belichenko PV, Dahlstrom A. Studies on the 3-dimensional architecture of dendritic spines and varicosities in human cortex by confocal laser scanning microscopy and Lucifer yellow microinjections. *J Neurosci Methods* 1995; 57: 55–61.
- Belichenko PV, Sourander P, Malmgren K, Nordborg C, von Essen C, Rhydenhag B, et al. Dendritic morphology in epileptogenic cortex from TRPE patients, revealed by intracellular Lucifer Yellow microinjection and confocal laser scanning microscopy. *Epilepsy Res* 1994; 18: 233–47.
- Blumcke I, Spreafico R, Haaker G, Coras R, Kobow K, Bien CG, et al. Histopathological findings in brain tissue obtained during epilepsy surgery. *N Engl J Med* 2017; 377: 1648–56.
- Blümcke I, Thom M, Aronica E, Armstrong DD, Vinters HV, Palmini A, et al. The clinicopathologic spectrum of focal cortical dysplasias: a consensus classification proposed by an ad hoc Task Force of the ILAE Diagnostic Methods Commission. *Epilepsia* 2011; 52: 158–74.
- Blumcke I, Züschratter W, Schewe JC, Suter B, Lie AA, Riederer BM, et al. Cellular pathology of hilar neurons in Ammon's horn sclerosis. *J Comp Neurol* 1999; 414: 437–53.
- Cepeda C, Hurst RS, Flores-Hernandez J, Hernandez-Echeagaray E, Klapstein GJ, Boylan MK, et al. Morphological and electrophysiological characterization of abnormal cell types in pediatric cortical dysplasia. *J Neurosci Res* 2003; 72: 472–86.
- Chapleau CA, Calfa GD, Lane MC, Albertson AJ, Larimore JL, Kudo S, et al. Dendritic spine pathologies in hippocampal pyramidal neurons from Rett syndrome brain and after expression of Rett-associated MECP2 mutations. *Neurobiol Dis* 2009; 35: 219–33.
- Crino PB. A pathogenic signaling pathway in developmental brain malformations. (Review). *Trends Mol Med* 2011; 17: 734–42.
- D’Gama AM, Woodworth MB, Hossain AA, Bizzotto S, Hatem NE, LaCoursiere CM, et al. Somatic Mutations activating the mTOR pathway in dorsal telencephalic progenitors cause a continuum of cortical dysplasias. *Cell Rep* 2017; 21: 3754–66.
- Ellender TJ, Raimondo JV, Irkle A, Lamsa KP, Akerman CJ. Excitatory effects of parvalbumin-expressing interneurons maintain hippocampal epileptiform activity via synchronous afterdischarges. *J Neurosci* 2014; 34: 15208–22.
- Engel JJ, Van Ness P, Rasmussen TB, Ojemann LM, Outcome with respect to epileptic seizures. New York, NY: Raven Press; 1993. p. 553–71.
- Fiala JC, Harris KM. Dendrite structure. In: G Stuart, N Spruston, M Hausse, editors. *Dendrites*. Oxford: Oxford University Press; 1999. p. 1–34.
- Fiala JC, Spacek J, Harris KM. Dendritic spine pathology: cause or consequence of neurological disorders? (Review). *Brain Res* 2002; 39: 29–54.
- Freiman TM, Eismann-Schweimier J, Froscher M. Granule cell dispersion in temporal lobe epilepsy is associated with changes in dendritic orientation and spine distribution. *Exp Neurol* 2011; 229: 332–8.
- Garbelli R, Munari C, De Biasi S, Vitellaro-Zuccarello L, Galli C, Bramero M, et al. Taylor's cortical dysplasia: a confocal and ultrastructural immunohistochemical study. *Brain Pathol* 1999; 9: 445–61.
- Glaser EM, Van der Loos H. Analysis of thick brain sections by obverse-reverse computer microscopy: application of a new, high clarity Golgi-Nissl stain. *J Neurosci Methods* 1981; 4: 117–25.
- Hinton VJ, Brown WT, Wisniewski K, Rudelli RD. Analysis of neocortex in three males with the fragile X syndrome. *Am J Med Genet* 1991; 41: 289–94.
- Huttenlocher PR, Heydemann PT. Fine structure of cortical tubers in tuberous sclerosis: a Golgi study. *Ann Neurol* 1984; 16: 595–602.
- Iffland PH, Crino PB. The role of somatic mutational events in the pathogenesis of epilepsy. (Review). *Curr Opin Neurol* 2019; 32: 191–7.
- Isokawa M. Preservation of dendrites with the presence of reorganized mossy fiber collaterals in hippocampal dentate granule cells in patients with temporal lobe epilepsy. *Brain Res* 1997; 744: 339–43.
- Isokawa M, Levesque MF. Increased NMDA responses and dendritic degeneration in human epileptic hippocampal neurons in slices. *Neurosci Lett* 1991; 132: 212–6.
- Isokawa M, Levesque M, Fried I, Engel J Jr. Glutamate currents in morphologically identified human dentate granule cells in temporal lobe epilepsy. *J Neurophysiol* 1997; 77: 3355–69.
- Jaworski J, Sheng M. The growing role of mTOR in neuronal development and plasticity. (Review). *Mol Neurobiol* 2006; 34: 205–19.
- Jehi L. The Epileptogenic Zone: concept and Definition. (Review). *Epilepsy Curr* 2018; 18: 12–6.
- Kasper BS, Stefan H, Buchfelder M, Paulus W. Temporal lobe microdysgenesis in epilepsy versus control brains. *Neuropathol Exp Neurol* 1999; 58: 22–8.
- LaSarge CL, Danzer SC. Mechanisms regulating neuronal excitability and seizure development following mTOR pathway hyperactivation. (Review). *Front Mol Neurosci* 2014; 7: 18.
- Machado-Salas JP. Abnormal dendritic patterns and aberrant spine development in Bourneville's disease – a Golgi survey. *Clin Neuropathol* 1984; 3: 52–8.
- Marsan E, Baulac S. Review: mechanistic target of rapamycin (mTOR) pathway, focal cortical dysplasia and epilepsy. (Review). *Neuropathol Appl Neurobiol* 2018; 44: 6–17.
- Medici V, Rossini L, Deleo F, Tringali G, Tassi L, Cardinale F, et al. Different parvalbumin and GABA expression in human epileptogenic focal cortical dysplasia. *Epilepsia* 2016; 57: 1109–19.
- Multani P, Myers RH, Blume HW, Schomer DL, Sotrel A. Neocortical dendritic pathology in human partial epilepsy: a quantitative Golgi study. *Epilepsia* 1994; 35: 728–36.
- Rossini L, Garbelli R, Gnatkovsky V, Didato G, Villani F, Spreafico R, et al. Seizure activity per se does not induce tissue damage markers in Human Neocortical Focal Epilepsy. *Ann Neurol* 2017; 82: 331–41.
- Scheibel ME, Crandall PH, Scheibel AB. The hippocampal–dentate complex in temporal lobe epilepsy. *Epilepsia* 1974; 15: 55–80.
- Sholl DA. Dendritic organization in the neurons of the visual and motor cortices of the cat. *J Anat* 1953; 87: 387–406.
- Sim NS, Ko A, Kim WK, Kim SH, Kim JS, Shim KW, et al. Precise detection of low-level somatic mutation in resected epilepsy brain tissue. *Acta Neuropathol* 2019; 138: 901–12.
- Spruston N. Pyramidal neurons: dendritic structure and synaptic integration. *Nat Rev Neurosci* 2008; 9: 206–21.
- Swann JW, Al-Noori S, Jiang M, Lee CL. Spine loss and other dendritic abnormalities in epilepsy. (Review). *Hippocampus* 2000; 10: 617–25.
- Tavazoie SF, Alvarez VA, Ridenour DA, Kwiatkowski DJ, Sabatini BL. Regulation of neuronal morphology and function by the tumor suppressors Tsc1 and Tsc2. *Nat Neurosci* 2005; 8: 1727–34.
- Torres MD, Garcia O, Tang C, Busciglio J. Dendritic spine pathology and thrombospondin-1 deficits in Down syndrome. *Free Radic Biol Med* 2018; 114: 10–4.
- Vaquero J, Qya S, Cabezudo JM, Bravo G. Morphological study of human epileptic dendrites. *Neurosurgery* 1982; 10: 720–4.
- von Campe G, Spencer DD, Lanerolle NC. Morphology of dentate granule cells in the human epileptogenic hippocampus. *Hippocampus* 1997; 7: 472–88.
- Wisniewski KE, Segan SM, Miezieski CM, Sersen EA, Rudelli RD. The Fra(X) syndrome: neurological, electrophysiological and neuropathological abnormalities. *Am J Med Genet* 1991; 38: 476–80.
- Wong M. Modulation of dendritic spines in epilepsy: cellular mechanisms and functional implications. (Review). *Epilepsy Behav* 2005; 7: 569–77.
- Wong M, Guo AD. Dendritic spine pathology in epilepsy: cause or consequence? (Review). *Neuroscience* 2013; 251: 141–50.

- World Health Organization. Epilepsy fact sheet. Geneva; 2017 (<http://www.who.int/mediacentre/factsheets/fs999/en/>).
- Xu X, Miller EC, Pozzo-Miller L. Dendritic spine dysgenesis in Rett syndrome. *Front Neuroanat* 2014; 10: 8–97.
- Ying Z, Wang I, Blümcke I, Bulacio J, Alexopoulos A, Jehi L, et al. A comprehensive clinico-pathological and genetic evaluation of bottom-of-sulcus focal cortical dysplasia in patients with difficult-to-localize focal epilepsy. *Epileptic Disord* 2019; 21: 65–77.
- Zaqout S, Kaindl AM. Golgi-Cox Staining Step by Step. *Front Neuroanat* 2016; 10: 38.
- Zucca I, Milesi G, Medici V, Tassi L, Didato G, Cardinale F, et al. Type II focal cortical dysplasia: Ex vivo 7T magnetic resonance imaging abnormalities and histopathological comparisons. *Ann Neurol* 2016; 79: 42–58. 10.1002/ana.24541